# Targeting LMO2 with a Peptide Aptamer Establishes a Necessary Function in Overt T-Cell Neoplasia

Alex Appert,[1,2] Chang-Hoon Nam,[1,4] Natividad Lobato,[1,5] Eva Priego,[3,6] Ricardo Nunez Miguel,[3] Tom Blundell,[3] Lesley Drynan,[1] Helen Sewell,[7] Tomoyuki Tanaka,[1,7] and Terence Rabbitts[1,7]

[1]Medical Research Council Laboratory of Molecular Biology; [2]Division of Molecular Histopathology, Department of Pathology, University of Cambridge, Addenbrooke's Hospital; [3]Department of Biochemistry, University of Cambridge, Cambridge, United Kingdom; [4]Korea Institute of Science and Technology Europe, Forschungsgesellschaft mbH, Saarbrücken, Germany; [5]Oryzon, Parc Cientific de Barcelona, Barcelona, Spain; [6]Instituto de Química Médica (Consejo Superior de Investigaciones Cientificas), Madrid, Spain; and [7]Leeds Institute of Molecular Medicine, St. James's University Hospital, University of Leeds, Leeds, United Kingdom

## Abstract

**LMO2 is a transcription regulator involved in human T-cell leukemia, including some occurring in X-SCID gene therapy trials, and in B-cell lymphomas and prostate cancer. LMO2 functions in transcription complexes via protein-protein interactions involving two LIM domains and causes a pre-leukemic T-cell development blockade followed by clonal tumors. Therefore, LMO2 is necessary but not sufficient for overt neoplasias, which must undergo additional mutations before frank malignancy. An open question is the importance of LMO2 in tumor development as opposed to sustaining cancer. We have addressed this using a peptide aptamer that binds to the second LIM domain of the LMO2 protein and disrupts its function. This specificity is mediated by a conserved Cys-Cys motif, which is similar to the zinc-binding LIM domains. The peptide inhibits Lmo2 function in a mouse T-cell tumor transplantation assay by preventing Lmo2-dependent T-cell neoplasia. Lmo2 is, therefore, required for sustained T-cell tumor growth, in addition to its preleukemic effect. Interference with LMO2 complexes is a strategy for controlling LMO2-mediated cancers, and the finger structure of LMO2 is an explicit focus for drug development.** [Cancer Res 2009;69(11):4784–90]

## Introduction

The molecular cloning of chromosomal translocation junctions and cDNA copies of genes affected by the chromosomal translocations resulted in the definition of how these abnormal chromosomes affect tumorigenesis (reviewed in ref. 1). Chromosomal translocations in T-cell acute leukemia (T-ALL) involving chromosome 11, band p13, resulted in the isolation of *LMO2* gene (2, 3), which belongs to a family of four genes, encoding small LIM-only proteins, in which *LMO1* is also involved in chromosomal translocations in T-ALL (4, 5). LMO1 and LMO2 affect T-ALL by interfering with T-cell differentiation before the appearance of overt T-cell neoplasia (6–11). Recently, LMO2 has been further implicated in T-ALLs arising after retroviral insertion during gene therapy trials for correcting the X-SCID defect (12–15). Overall, expression of LMO2 in T-ALL is much greater than simply due to chromosomal translocations (16, 17) and includes cryptic deletions of 11p13 (18), but it remains unknown if LMO2 is only required for development and tumor continuation.

LMO2 is a T-cell oncogenic protein, but its normal role is in controlling cell fate in normal hematopoiesis, being required for primitive and definitive hematopoiesis (19–21). In addition, there is a role for LMO2 in endothelial cell remodeling (22). The *LMO2* gene encodes a 156–amino acid protein, comprising two zinc-binding LIM domains, each with two LIM fingers. The LIM fingers, separated by two amino acids, comprises a zinc-binding motif of either four cysteines or three cysteines plus a histidine or aspartate residue coordinating the zinc atom and a finger of ~16 to 20 residues (represented in Supplementary Fig. S1*B*). LIM domains function in protein-protein interactions rather than direct DNA binding (23–25). LMO2 can bind to TAL1/SCL (another T-ALL translocation-associated protein), LDB1, and GATA-1 in a DNA-binding complex found in erythroid cells (26). This complex recognizes a bipartite DNA site, comprising an E box separated from a GATA site by ~12 bp (26). In studies of T-cell tumors arising in an *Lmo2* gain-of-function transgenic mouse model, an analogous Lmo2-associated complex was detected, but in this case binds a bipartite sequence comprising tandem E boxes (27). In addition, other protein interaction partners are known (28), including the retinoblastoma protein (29).

The frequent expression of LMO2 in T-ALL poses LMO2 protein as an intriguing therapy target, and its involvement in transcription complexes provides the focus of applications that can produce a therapeutic effect. In addition, the protein is expressed in diffuse large B-cell lymphoma, wherein it has prognostic significance (30–32), and is also found overexpressed in prostate tumors (33). Whereas protein-protein interactions have been thought to be "undruggable," this dogma is being questioned (34) by clear examples of molecules that can indeed induce a therapeutic effect in preclinical mouse models. In addition, our recent work with macrodrugs that bind to RAS indicates that interfering with protein interactions within the cell has a preclinical therapeutic index (35).

One of the most promising ways that drug design can be focused on is using structural data to model shapes that can be transmuted into chemicals. In those cases wherein no structure is available, antibody fragments or peptide aptamers can serve as guides to functionally relevant parts of target proteins, wherein small molecules can have an effect. Therefore, macrodrugs can serve as lead compounds for rational or *in silico* design of new small molecule mimetics. We have found that an antibody fragment in the single-chain Fv format (VH linked to VL) can block the function of LMO2 in a mouse tumor model (36) but the size of the single-chain Fv format surface, which is occupied on the LMO2 target, is too big

**Note:** Supplementary data for this article are available at Cancer Research Online (http://cancerres.aacrjournals.org/).

A. Appert and C-H. Nam made equal contributions to the study.

**Requests for reprints:** Terence H. Rabbitts, Leeds Institute of Molecular Medicine, St. James's University Hospital, Leeds, LS9 7TF, United Kingdom. Phone: 44-113-343-8518; Fax: 44-113-343-8601; E-mail: thr@leeds.ac.uk.



doi:10.1158/0008-5472.CAN-08-4774

to determine the key interaction sites. We have now developed the peptide aptamer that binds specifically to LMO2 and prevents its function as a T-cell oncogenic protein in a mouse transplantation assay. Genetic and *in silico* modeling shows that the peptide binds to the fourth LIM finger at the point wherein the zinc atom resides and exerts its therapeutic effect by interference with the stability of the second LIM domain. This location is a target for drug design.

## Materials and Methods

**Screening a peptide aptamer library with LMO2.** A truncated form of LMO2 (amino acids 28–150) was fused to the LexA DNA binding domain in a modified version of pBTM116, in which the selectable marker for yeast *TRP1* had been replaced by the *LEU2* gene, allowing growth in a medium lacking leucine. This *LexA-LMO2* construct was used as a bait to screen $3 \times 10^6$ transformants from a 20-mer peptide library (37) using the L40 yeast strain and following the protocol described (38). In this library (cloned in a vector with *TRP1*), which contains $>10^9$ initial members, the active site loop of *Escherichia coli* thioredoxin (TRX) is used as the scaffold to display the 20-mer peptides.

**Mammalian two-hybrid assays.** TRX peptide and the truncated LMO2 bait (amino acids 28–150) segments were subcloned into the mammalian pEF-VP16 vector as a fusion with the VP16 activation domain or into the pM vector (39) as a fusion with the Gal4 DNA-binding domain. The interaction between LMO2 and the peptides was tested in Chinese hamster ovary (CHO) cells using the dual-luciferase reporter assay system (Promega) according to the manufacturer's instructions. All luminescence values by *firefly* luciferase were normalized against the values by *Renilla* luciferase.

The best interacting peptide (PA207) was subcloned intact or as truncated versions in the pM vector, giving the fusion with the Gal4DBD directly or indirectly through a flexible linker consisting of three repeats of Gly-Gly-Gly-Gly-Ser. The mutated LMO2 preys have been described (36).

**Protein purification and surface plasmon resonance.** Recombinant protein expression, purification, and surface plasmon resonance analysis are described in the Supplementary Data.

**Retrovirus infection into *Lck-Lmo2* tumor T cells.** A PCR fragment from Gal4DBD-linker-PA207 (Gal4DBD-LPA207, 12-mer) was cloned into pMIG retroviral vector (40). PlatE viral packaging cells (41) were plated in six-well plates ($10^6$ per well) and transfected with 2 μg of pMIG-Gal4DBD-LPA207 or pMIG empty vector using 8 μL of FUGENE6 reagent (Roche) per well to produce viral supernatants. Neoplastic T cells prepared from the thymoma of *Lck-Lmo2* transgenic mice (36) were infected as described in the Supplementary Data.

**Transplantation of retrovirally infected cells into *Rag1* null recipients.** After retrovirus infections, the percentage of green fluorescent protein (GFP)–expressing infected cells was assessed using flow cytometry before transplantation. The mixed population ($2 \times 10^6$) were i.v. injected into *Rag1*$^{-/-}$ mice. Before transplantation, cell viability was measured by trypan blue exclusion. After the injection procedure, cell viability was again determined in the residual populations to ensure that injected cells were still viable. After ~6 wk, mice were sacrificed and GFP expression was analyzed in spleen cells by flow cytometry.

**Structural *in silico* analysis.** The LMO2 structural model with and without bound peptide was created *in silico* by comparative modeling using known structures of LIM proteins (42, 43). The detailed *in silico* modeling appears in the Supplementary Data.

## Results

**Anti-LMO2 peptide aptamers homologous to elements in LIM fingers.** A yeast peptide aptamer library (37) was screened in

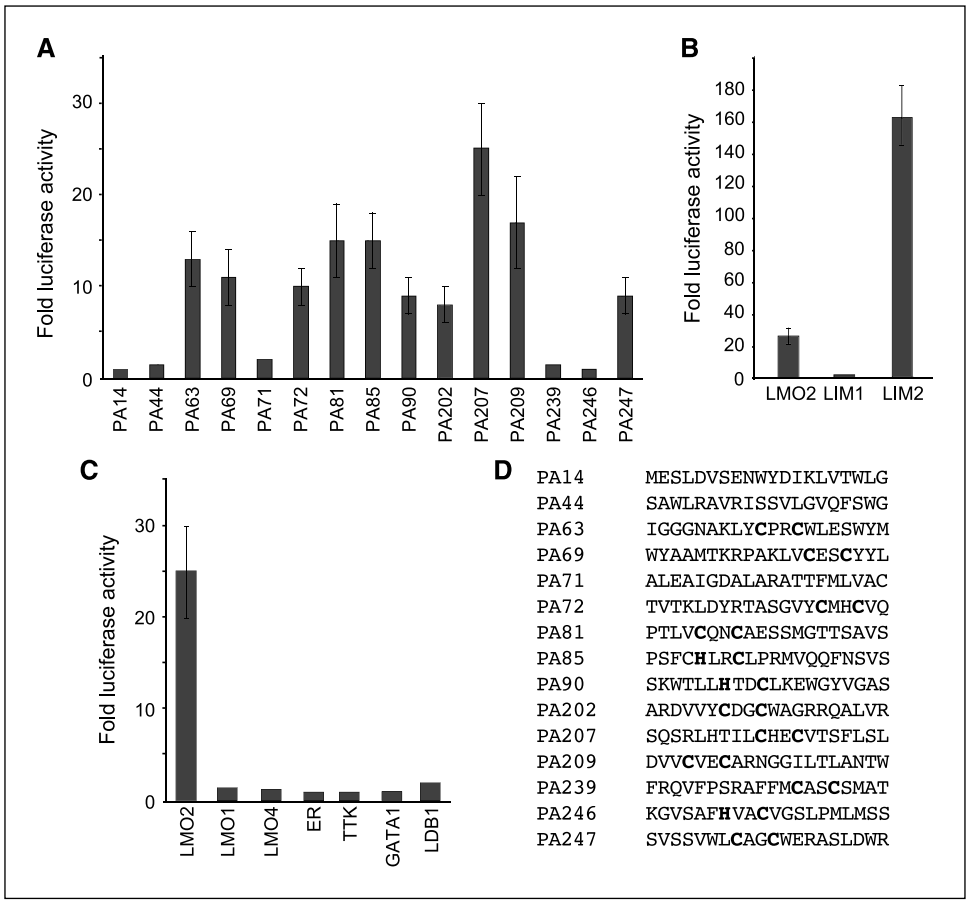


**Figure 1.** Binding properties of anti-LMO2 peptide aptamers. Fifteen peptide aptamers were isolated by a yeast two-hybrid screen and examined by CHO two-hybrid luciferase assays (*A–C*). *A,* the fold luciferase activation obtained by coexpression of a Gal4DBD-LMO2 fusion together with various peptide aptamer fusions with VP16 (TRX-PA14-VP16, etc). *B,* the fold luciferase activation obtained by coexpression of Gal4DBD-TRX-PA207 bait and LMO2-VP16 preys comprising either whole LMO2 (i.e., LIM1 + LIM2) or the LIM1 or LIM2 domains only. *C,* the fold luciferase activation obtained by coexpression of Gal4DBD-TRX-PA207 bait with preys comprising VP16 activation domain fusion with LMO family members (LMO1 and LMO4) or with zinc finger proteins, i.e., estrogen receptor α (*ER*; zinc finger type $C_4$), protein kinase (*TTK*; zinc finger type $C_2H_2$), and GATA1 (DNA binding protein). The interaction with LMO2 binding partner LDB1 was used as a negative control. *Error bars,* SD (minimum of three independent experiments). Fold luciferase activations are relative to cotransfection of prey or bait + empty vector. *D,* alignment of amino acid sequences (single-letter code) of TRX peptide aptamers isolated from the yeast two-hybrid screen.

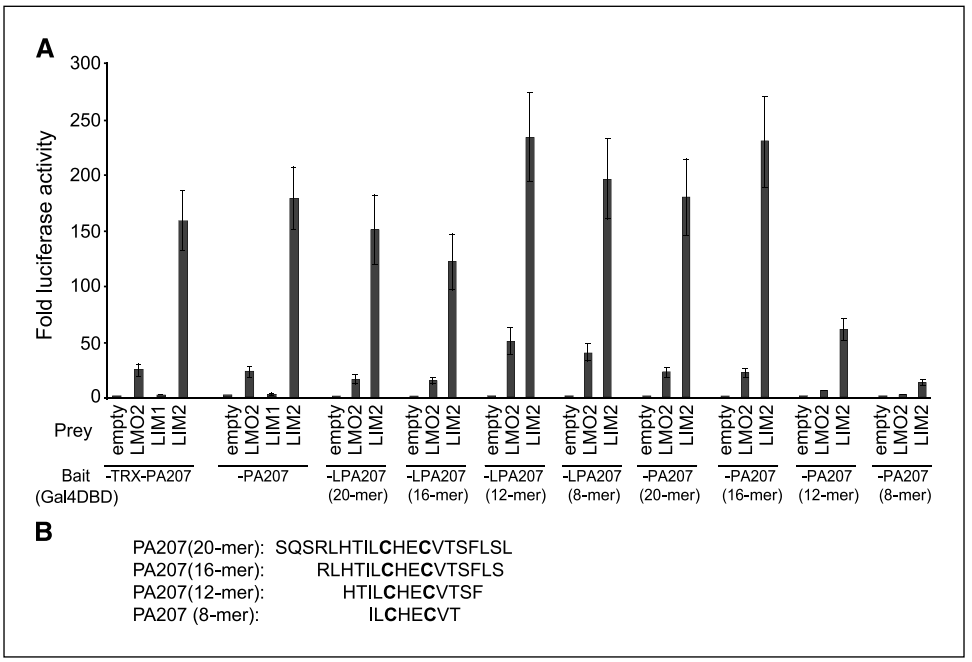


**Figure 2.** The lead peptide aptamer PA207 expressed at the COOH terminus of the Gal4DBD retains interaction with LMO2. *A,* CHO cells were transfected with plasmids expressing various baits, Gal4DBD-PA fusions and preys, comprising LMO2 (LIM1 + LIM2) or only the second LIM domain (LIM2) fused to the VP16 activation domain, together with luciferase reporters. The fold luciferase activation is normalized for the activity of Gal4DBD-PA207 without prey. Three different PA207 expression clones were transfected in the CHO luciferase assay respectively, Gal4DBD-TRX-PA207, Gal4DBD-PA207 (peptide aptamers length varies from 20 to 8 amino acids as indicated), or Gal4DBD-linker-PA207 (Gal4DBD-LPA207, peptide aptamers length varies from 20 to 8 amino acids as indicated), together with LMO2(LIM1 + LIM2)-VP16, LIM1-VP16, or LIM2-VP16 as indicated. *B,* alignment of amino acids sequences (single-letter codes) of truncated PA207 peptide aptamers.

yeast with an LMO2 bait. The yeast peptide aptamer library consisted of a diverse set of clones expressing random peptides (20-mer) incorporated into the scaffold of bacterial TRX protein as an external loop. Transformans ($3 \times 10^6$) were screened, and 15 were confirmed to be LMO2-specific binders. These clones were tested in a mammalian two-hybrid luciferase assay, and 10 showed a detectable reporter activity for LMO2 (Fig. 1*A*). The sequences of the peptides revealed the presence of a motif Cys-X-X-Cys or His-X-X-Cys in 12 of the clones (Fig. 1*D*). The similarity of this peptide motif to the zinc-binding regions of LMO2 (Supplementary Fig. S1*B* online) indicates that the peptides bind to LMO2 at a zinc atom coordination site.

A conserved region extends a few residues on either of the core Cys/His-x-x-Cys motif, with generally two hydrophobic residues on the $NH_2$ terminal side and one hydrophobic residue on the COOH terminal side of the core motif. Furthermore, a charged amino acid often occurs as one of the two amino acids between Cys/His and Cys (Fig. 1*D*).

**The lead anti-LMO2 peptide aptamer binds to the second LIM domain.** The binding site of TRX-PA207 on LMO2 was assessed using variant forms of LMO2 protein. CHO cells were cotransfected with plasmids expressing TRX-PA207 fused to the Gal4DBD (Gal4DBD-TRX-PA207) and LMO2(LIM1 + LIM2), LMO2(LIM1), or LMO2(LIM2) fused to VP16 (prey) with luciferase reporter plasmids (Fig. 1*B*). The luciferase activation with the LMO2(LIM1 + LIM2) prey and LMO2(LIM2) were stimulated by 25-fold and 160-fold, respectively, whereas the LMO2(LIM1) prey was inactive showing that TRX-PA207 binds to the second LIM domain of LMO2 (i.e., LIM2).

We assessed cross-reaction of the PA207 peptide aptamer with other LIM-only family members and with other zinc-binding proteins (Fig. 1*C*). Significant binding was only found with LMO2 and not with the other LIM-only or zinc finger proteins or the LIM-binding protein LDB1. The LIM domain is most closely related to the DNA-binding domain of the GATA fingers, but no appreciable binding was found with a GATA1 bait. Finally, the anti-LMO2 peptide aptamer is specific for the LIM fingers, as TRX-PA207 showed no binding to the zinc fingers of estrogen receptor α (zinc finger type $C_4$) or the protein kinase TTK (zinc finger type $C_2H_2$; Fig. 1*C*).

We determined if the peptide could bind LMO2 in a semiconstrained form by expressing the peptide linked as a COOH terminal sequence fused with the Gal4DBD (bait). We used either a protein comprising Gal4DBD fused with the whole TRX-PA207 (Gal4DBD-TRX-PA207; Fig. 2*A*) with a Gly-Ser flexible linker (Gal4DBD-TRX-LPA207) or comprising Gal4DBD fused with just the 20 amino acids of the PA207 (Gal4DBD-PA207) with preys comprising whole LMO2 (LIM1 + LIM2), the LIM1, or the LIM2 domain only. Both baits behaved equivalently in luciferase production, indicating binding to the LIM2 domain–only prey with greatest efficiency. Both fully constrained (Gal4DBD-TRX-PA207) and semiconstrained (Gal4DBD-PA207) baits had identical binding to LMO2; thus, PA207 is able to meet its target site on LMO2 with only $NH_2$ terminal linkage to the DBD carrier.

We assessed the required number of flanking amino acids needed for the binding by comparing four peptides as baits (Fig. 2*B*). High-luciferase stimulation was observed with both formulations of bait with the LIM2 domain prey, and when the linker was present, the PA207 of 12 or 8 amino acids was able to bind with the prey [-LPA207 (12 mer) or (8 mer); Fig. 2*A*]. Conversely, the direct fusion of Gal4DBD with PA207 resulted in diminished binding for peptide lengths of 12 or 8. This suggests that steric hindrance prevents the latter from having access to the LMO2 protein.

**The conserved Cys-x-x-Cys motif of the peptide is required to bind LIM finger 4.** Because LIM2 has the greatest binding with PA207, it suggests that the tertiary structure of LMO2 limits access to the peptide. Further definition of the PA207 binding on LIM2 domain was achieved with a series of LIM finger mutants with each side of each LIM finger changed to either the LIM sequences of ISL1 or LMO4 (36). These preys were coexpressed with the Gal4DBD-LPA207(12-mer) bait in the two-hybrid assay, and their relative expression levels were determined (Fig. 3*A*). The luciferase analysis showed the most significant effect with the mutant in which the right side of finger 4 (Fig. 3*A*) was changed into the

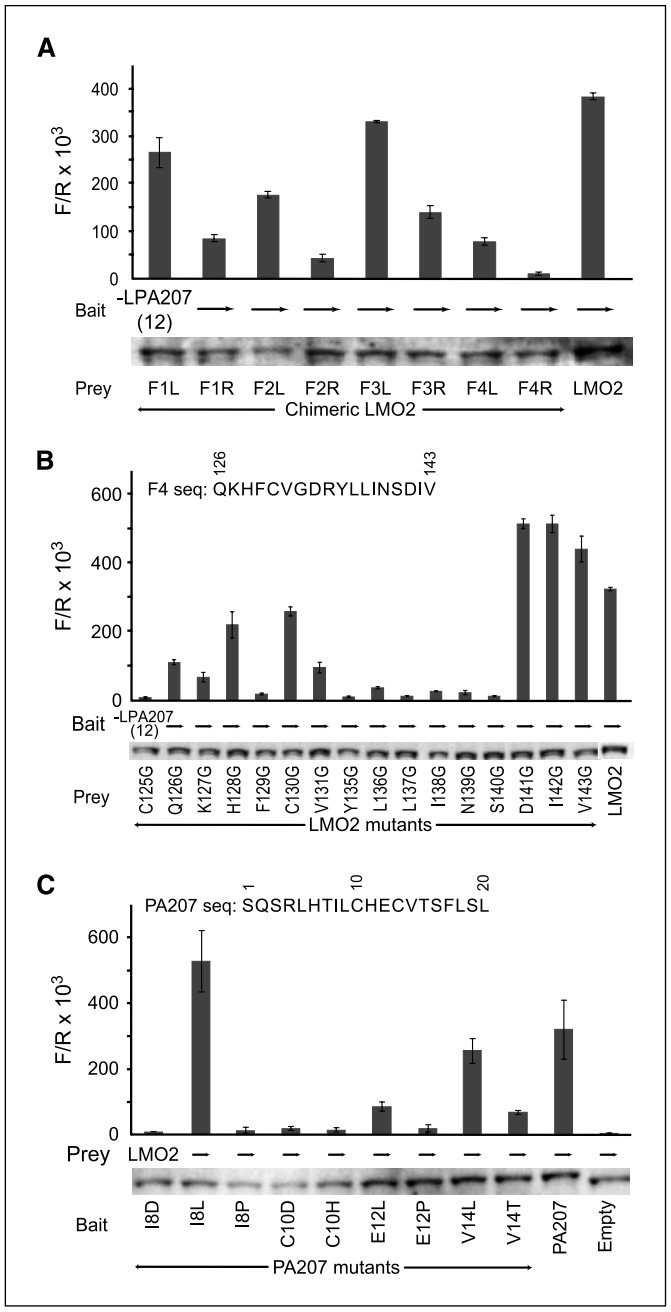


**Figure 3.** Mutagenesis of LMO2 to determine PA207 binding site. Luciferase reporter assays in CHO cells were carried out to delineate the binding site of the PA207 peptide with LMO2 LIM fingers. *A,* chimeric LIM finger preys with ISL1 or LMO4 finger sequences grafted into LMO2 and fused to the VP16 activation domain (*L,* left side sequence; *R,* right side sequence) were coexpressed with the Gal4DBD-LPA207 bait (12-mer; ref. 36). The expression levels of the mutant LMO2 proteins were established by Western detection with an anti-VP16 antibody (*bottom*). *B,* luciferase reporter assays using single–amino acid mutations in LMO2 LIM finger 4. The LMO2 proteins were expressed as VP16 prey fusions (Western detection by an anti-VP16 antibody is at the bottom) together with Gal4DBD-LPA207 bait. The F4 sequence is the LMO2 finger 4. The preys on the *x* axis indicate glycine mutants of LMO2 in each residue from C125G to V143G. *C,* luciferase reporter assays using single–amino acid mutations in the PA207 peptide (20-mer) sequence. Gal4DBD-linker-PA207 proteins with amino acid substitutions in the LMO2 recognition peptide were expressed as Gal4DBD-LPA207 bait fusions (Western detection by anti-Gal4DBD antibody) together with LMO2-VP16 prey. The baits on the *x* axis indicate point mutants of PA207 (20-mer) in each residue from I8D to V14T. *Error bars,* SD (minimum of three experiments). *Y* axis shows the ratio of *firefly* (*F*) and *Renilla* (*R*) luciferase activity relative to cotransfection of prey or bait + empty vector. The PA207 sequence is for the 20-mer original isolate.

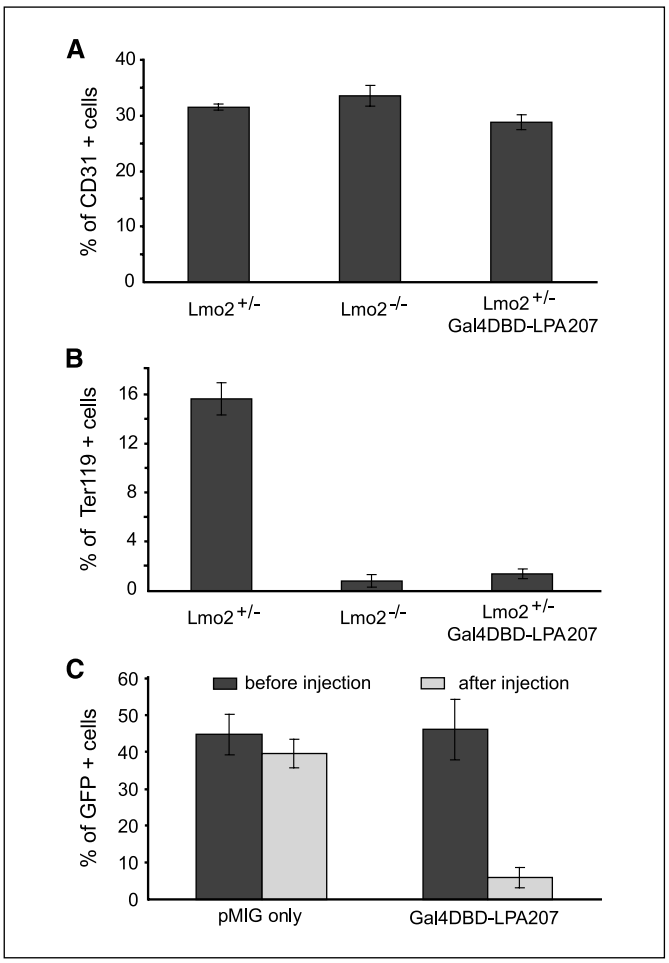


**Figure 4.** The peptide aptamer inhibits LMO2-dependent cellular functions. PA207 has an inhibitory effect on Lmo2 *in vivo* function in erythropoietic (*A* and *B*) and T-cell neoplasia (*C*) assays. The ES clones used in the erythropoietic assay were heterozygous *Lmo2* (with a *lacZ* gene knocked-in *Lmo2*; ref. 19) designated either $Lmo2^{+/-}$; null *Lmo2* ES cells ($Lmo2^{-/-}$) or the latter ES cells expressing Gal4DBD-LPA207 (*Lmo2*+/−; Gal4-DBD-LPA207). Embryoid bodies (11 d) were used to quantify cells expressing the endothelial marker CD31 (*A*) or the erythroid marker Ter119 (*B*). *C,* neoplastic T cells from *Lck-Lmo2* transgenic mice transplant into *Rag1* null mice (36). T cells were transduced with retrovirus expressing GFP only or expressing Gal4DBD-LPA207 (12-mer) fusion protein and GFP. The percentage of transduced cells was determined by flow cytometry before transplantation into *Rag1* recipients (*closed boxes*). Recipient mice were sacrificed at signs of ill health, and percentage of GFP-positive spleen cells was assessed by flow cytometry (*gray boxes*). *Error bars,* SD of three independent experiments.

LMO4 sequence. In this mutant, no significant binding to PA207 was observed.

Mutations were made at each residue through the "right-hand" side of finger 4 (sequence in Supplementary Fig. S1 online), and the luciferase stimulation was determined with the Gal4DBD-LPA207 (12-mer) bait (Fig. 3*B*). Substitution of the Cys125 (involved in zinc coordination in finger 4) removed PA207 interaction, suggesting that the peptide aptamer binding site is the zinc-binding Cys-x-x-Cys motif of the LIM finger 4. Mutation of nonzinc binding finger 4 residues 128 and 130 decreased the reporter activity (Fig. 3*B*), whereas mutation of finger 4 residues 135 to 140 significantly decreased their binding activities to PA207. An important residue in the LMO2 protein also seems to be phenylalanine (residue 129), as changing at that position to glycine ablates peptide binding (Fig. 3*B*). The amino acids of the PA207 that have key interactions

were similarly assessed by mutagenesis (Fig. 3*C*). Changing the cysteine residue 10 of PA207 to aspartate or histidine destroys binding, as does changing isoleucine (residue 8) to either aspartic acid or proline (but not the conserve change to leucine).

We have determined the binding affinity of PA207 with LMO2 *in vitro* using surface plasmon resonance with recombinant protein (i.e., GST-LMO2 and HIS-TRX-PA207; Supplementary Fig. S2). Using different concentrations of TRX-PA207 protein, the average Kd for binding was calculated as 29 nmol/L.

**The peptide aptamer inhibits LMO2 protein function.** LMO2 is a protein interaction module (26, 27, 44–46) that operates by protein interaction in each of its functional settings, which includes hematopoiesis, angiogenesis, and leukemogenesis (8, 28, 47). Gene targeting approaches showed that *Lmo2* null ES cells fail to undergo differentiation into erythroid (Ter119-expressing) cells, whereas *de novo* formation of endothelial (CD31-expressing) cells is unimpeded (21). We used ES cells in which *Lmo2* has been disrupted by knock in of the *lacZ* gene into one allele (21) to stably transfect with a plasmid which expressed Gal4DBD-LPA207. We observed that the PA207 had no effect on CD31-positive cell development (Fig. 4*A*), whereas it has an inhibitory effect on development of Ter119-expressing cells mimicking the $Lmo2^{-/-}$ ES cells (Fig. 4*B*). Therefore, the peptide aptamer binds to Lmo2 complexes and prevents specific function.

The effectiveness of the PA207 in LMO2-dependent tumorigenic models was analyzed using a preclinical mouse transplantation assay (36). Neoplastic T cells from an Lmo2-dependent transgenic mouse model were infected with retrovirus expressing the Gal4DBD-LPA207 and GFP reporter or vector only–expressing GFP. The proportion of infected cells was assessed using flow cytometry (Fig. 4*C*), and these populations were transplanted into mature lymphocyte-null *Rag1* knockout mice. Spleen cells were collected from mice with splenomegaly, and the proportion of GFP-expressing cell was determined. A 90% reduction of GFP-positive neoplastic T cells was observed in the recipients that were transplanted with cells infected with retrovirus encoding PA207 (Fig. 4*C*) compared with those only expressing GFP (vector-only infections). These data are indicative of the specific growth inhibition of the neoplastic cells by PA207 *in vivo* in tumor-bearing mice.

***In silico* modeling of LMO2 and peptide aptamer binding.** To build a model of the protein-peptide interaction, an *in silico* model of LMO2 was generated using mouse Lmo4 and partial mouse Lmo2 structural data (42, 43). Our *in silico* model indicates that the

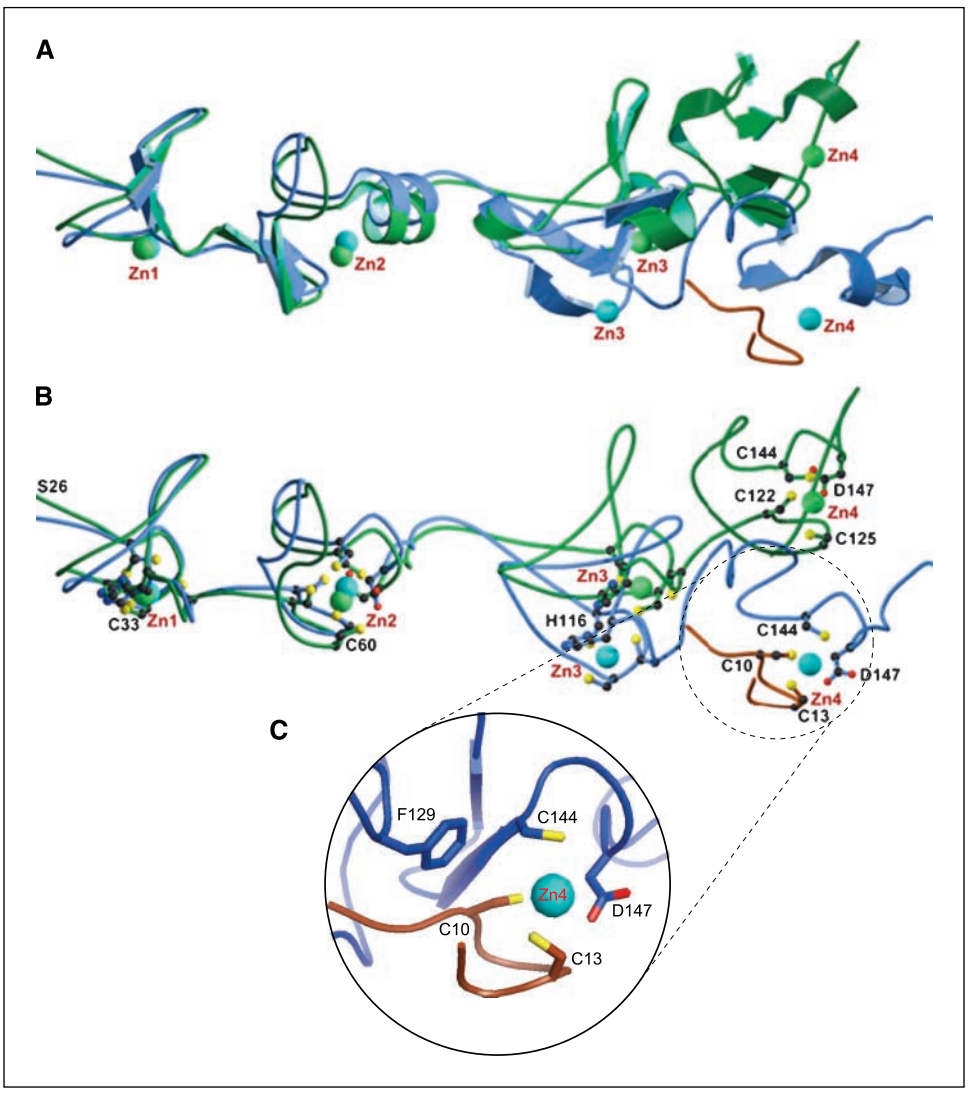


**Figure 5.** *In silico* modeling of LMO2 and LMO2-peptide complex. *A, in silico* representation of the human LMO2 protein (*green*) overlaid with LMO2 with bound PA207 (8-mer; LMO2 is in blue and PA207 is in brown). Zinc atoms are in green and blue spheres. *B,* a ribbon representation of the above. Side chain of residues involved in the binding to Zn shown as sticks with the individual residue numbers (*yellow,* sulfur atoms; *black,* carbon atoms; *red,* oxygen atoms). Individual residues correspond to the sequence in Supplementary Fig. S1*A*. *C,* magnification of interaction region of LMO2 and PA207.

peptide PA207 8-mer (sequence ILCHECVT) has similarities to the region of the LMO2 LIM2 finger 4 sequence FKCAACQK, which is itself responsible for binding the fourth zinc atom (residues 120 to 127; Supplementary Fig. S1 online). The most likely position for the peptide binding site is where the fourth Zn atom is in LMO2 (Fig. 5). The zinc atom of finger 4 seems to be the most exposed and may explain the interaction of the peptide at this position rather than the other three zinc atoms. A model was built carrying the LMO2 point mutation with phenylalanine to glycine in the codon 129 (F129G), indicating a distortion of the region-binding zinc. The phenylalanine is exposed to the peptide interaction, whereas the glycine is buried in the F129G mutant and the zinc atom of finger 4 is correspondingly less exposed (Supplementary Fig. S3), providing an *in silico* explanation for the effect of the F129G mutation on PA207 interaction with LMO2.

## Discussion

**LMO2 binding peptides target the zinc binding region of the LIM2 domain.** The LMO2-binding peptides were selected from a random 20-mer library in the TRX scaffold (37), displayed binding through a Cys/His-x-x-Cys motif and preferential binding to the LMO2 LIM2 finger 4. Mutation of the cysteine residues in the peptide confirms the requirement for these residues (Fig. 3*C*), but other residues in the peptide have important interactions with LMO2, such as isoleucine residue 8 in PA207 (see Fig. 3*C*).

Our *in silico* model concurs with mutagenesis data and predicts that interaction with the peptide has structural consequences for the second LIM domain without direct changes to the first domain (Fig. 5). Thus, the mechanism by which the peptide elicits its effect on the biological role of LMO2 in the T-cell neoplasia assay may be by disrupting the transcription complex in which LMO2 is a bridging molecule.

**Inhibition of LMO2 function by peptide aptamer.** Our data show that the peptide aptamer (using the Gal4DBD scaffold) can prevent Lmo2-dependent T-cell neoplasia in a tumor transplant *in vivo* assay. This validates both PA207 and LMO2 sequences as important elements for any possible LMO2-based therapy. In addition, the PA207 replicates the effect of gene targeting knockout of *Lmo2*; thus, PA207 is an ideal reagent for investigating the normal LMO2 interactome. Cell-specific and temporal activation of the peptide aptamer would facilitate the dissection of properties of LMO2 transcription complexes in development.

The T-cell neoplasia transplant assay is a surrogate of T-cell neoplasia therapy. The results show that transplanted T cells expressing the PA207 macrodrug are severely growth impaired in the recipient mice, showing that Lmo2 functional activity is required for tumor maintenance in this mouse model. This means that LMO2 is a drug target for therapy of T-ALL and possibly other neoplasias, such as diffuse large B-cell lymphoma (30, 31) and prostate cancer (33), wherein aberrant LMO2 expression is reported. Furthermore, the peptide reported here will act as a lead for LMO2 drug development.

**LMO2 is a validated therapeutic target in T-cell neoplasia.** The Lmo2-dependent T-cell neoplasias that develop in the transgenic model occur as clonal tumors with long latency, showing that the *Lmo2* transgene is necessary but not sufficient for cancer. Neoplasia is preceded by an Lmo2-dependent period of partial blockade of T-cell differentiation at the immature T-cell stage. As previously argued (48), this blockade of T-cell differentiation coincides with the expression of the Rag recombinase, and so, in humans, the *LMO2* chromosomal translocations will occur at that stage, resulting in inhibition of differentiation of the afflicted T cell and eventual appearance of overt cancer. The question of whether LMO2 is needed only for this preleukemic stage or also for the overt neoplastic stage is answered by our studies with PA207, showing overt tumor inhibition by the macrodrug. Thus, LMO2 is a therapeutic target in LMO2-expressing T-cell leukemias and perhaps also B-cell lymphoma and prostate cancer where LMO2 is expressed.

Our molecular data locates LIM finger 4 as a key region of LMO2 that could be the focus of small molecule drug development to ablate the transcription complex. This approach can be tackled by development of a mimetic compound, either by selection processes that compete the binding of the LMO2-binding peptide or by *in silico* virtual drug screens using either the modeling of the LMO2-peptide complex or from structures that may be obtained in the future. The specificity for LMO2 LIM fingers is especially encouraging for this drug development endeavor and seems to rely of structural features of the LMO2 protein not shared by the family members.

## Disclosure of Potential Conflicts of Interest

No potential conflicts of interest were disclosed.

## Acknowledgments

Received 12/22/08; revised 2/19/09; accepted 3/20/09.

**Grant support:** Leukaemia Research Fund (United Kingdom), Medical Research Council (United Kingdom), and University of Leeds. A. Appert and C-H. Nam were part funded by Lady Tata Memorial Fund fellowships, H. Sewell is the recipient of an LRF Gordon Pillar studentship, and M.N. Lobato was part funded by an LRF fellowship. E.M. Priego was supported by a grant from the Spanish Ministerio de Educacion y Ciencia.

The costs of publication of this article were defrayed in part by the payment of page charges. This article must therefore be hereby marked *advertisement* in accordance with 18 U.S.C. Section 1734 solely to indicate this fact.

We thank Dr. R. Brent for the peptide aptamer yeast library and Professor T. Kitamura for the PlatE packaging cell line.

## References

1. Rabbitts TH. Chromosomal translocations in human cancer. Nature 1994;372:143–9.
2. Boehm T, Foroni L, Kaneko Y, Perutz MP, Rabbitts TH. The rhombotin family of cysteine-rich LIM-domain oncogenes: distinct members are involved in T-cell translocations to human chromosomes 11p15 and 11p13. Proc Natl Acad Sci U S A 1991;88:4367–71.
3. Royer-Pokora B, Loos U, Ludwig W-D. TTG-2, a new gene encoding a cysteine-rich protein with the LIM motif, is overexpressed in acute T-cell leukaemia with the t(11;14)(p13;q11). Oncogene 1991;6:1887–93.
4. Boehm T, Baer R, Lavenir I, et al. The mechanism of chromosomal translocation t(11;14) involving the T-cell receptor Cδlocus on human chromosome 14q11 and a transcribed region of chromosome 11p15. EMBO J 1988; 7:385–94.
5. McGuire EA, Davis AR, Korsmeyer SJ. T-cell translocation gene 1 (Ttg-1) encodes a nuclear protein normally expressed in neural lineage cells. Blood 1991; 77:599–606.
6. Fisch P, Boehm T, Lavenir I, et al. T-cell acute lymphoblastic lymphoma induced in transgenic mice by the RBTN1 and RBTN2 LIM-domain genes. Oncogene 1992;7:2389–97.
7. Larson R, Fisch P, Larson T, et al. T cell tumours with disparate phenotypes develop with long latency in mice transgenic for *rbtn2*. Oncogene 1994;9:3675–81.
8. Larson RC, Lavenir I, Larson TA, et al. Protein dimerisation between Lmo2 (Rbtn2) and Tal1 alters thymocyte development and potentiates T cell tumorigenesis in transgenic mice. EMBO J 1996;15:1021–7.

**9.** Larson RC, Osada H, Larson TA, Lavenir I, Rabbitts TH. The oncogenic LIM protein Rbtn2 causes thymic developmental aberrations that precede malignancy in transgenic mice. Oncogene 1995;11:853–62.

**10.** Neale GA, Rehg JE, Goorha RM. Ectopic expression of rhombotin-2 causes selective expansion of the thymus and T-cell tumours in transgenic mice. Blood 1995;86: 3060–71.

**11.** Neale GA, Rehg JE, Goorha RM. Disruption of T-cell differentiation precedes T-cell tumor formation in LMO2 (rhombotin-2) transgenic mice. Leukaemia 1997; 11:289–90.

**12.** Hacein-Bey-Abina S, von Kalle C, Schmidt M, et al. *LMO2*-associated clonal T cell proliferation in two patients after gene therapy for SCID-X1. Science 2003; 302:415–9.

**13.** Thrasher AJ, Gaspar HB, Baum C, et al. Gene therapy: X-SCID transgene leukaemogenicity. Nature 2006;443: E5–6; discussion B6–7.

**14.** Howe SJ, Mansour MR, Schwarzwaelder K, et al. Insertional mutagenesis combined with acquired somatic mutations causes leukemogenesis following gene therapy of SCID-X1 patients. J Clin Invest 2008; 118:3143–50.

**15.** Baum C, Schambach A, Modlich U, Thrasher A. [Gene therapy of SCID-X1]. Bundesgesundheitsblatt Gesundheitsforschung Gesundheitsschutz 2007;50:1507–17.

**16.** Ferrando AA, Look AT. Gene expression profiling in T-cell acute lymphoblastic leukemia. Semin Hematol 2003;40:274–80.

**17.** Ferrando AA, Neuberg DS, Dodge RK, et al. Prognostic importance of TLX1 (HOX11) oncogene expression in adults with T-cell acute lymphoblastic leukaemia. Lancet 2004;363:535–6.

**18.** Van Vlierberghe P, van Grotel M, Beverloo HB, et al. The cryptic chromosomal deletion del(11)(p12p13) as a new activation mechanism of LMO2 in pediatric T-cell acute lymphoblastic leukemia. Blood 2006;108: 3520–9.

**19.** Warren AJ, Colledge WH, Carlton MBL, Evans MJ, Smith AJH, Rabbitts TH. The oncogenic cysteine-rich LIM domain protein rbtn2 is essential for erythroid development. Cell 1994;78:45–58.

**20.** Visvader JE, Mao X, Fujiwara Y, Hahm K, Orkin SH. The LIM-domain binding protein Ldb1 and its partner LMO2 act as negative regulators of erythroid differentiation. Proc Natl Acad sci U S A 1997;94:13707–12.

**21.** Yamada Y, Warren AW, Dobson C, Forster A, Pannell R, Rabbitts TH. The T cell leukaemia LIM protein Lmo2 is necessary for adult mouse haematopoiesis. Proc Natl Acad Sci U S A 1998;95:3890–5.

**22.** Yamada Y, Pannell R, Rabbitts TH. The oncogenic LIM-only transcription factor Lmo2 regulates angiogenesis but not vasculogenesis. Proc Natl Acad Sci U S A 2000;97:320–4.

**23.** Schmeichel KL, Beckerle MC. The LIM domain is a modular protein-binding interface. Cell 1994;79:211–9.

**24.** Valge-Archer VE, Osada H, Warren AJ, et al. The LIM protein RBTN2 and the bHLH protein TAL1 are present in a complex in erythroid cells. Proc Natl Acad Sci U S A 1994;91:8617–21.

**25.** Wadman I, Li J, Bash RO, et al. Specific *in vivo* association between the bHLH and LIM proteins implicated in human T cell leukaemia. EMBO J 1994; 13:4831–9.

**26.** Wadman IA, Osada H, Grutz GG, et al. The LIM-only protein Lmo2 is a bridging molecule assembling an erythroid, DNA-binding complex which includes the TAL1, E47, GATA-1 and Ldb1/NLI proteins. EMBO J 1997;16:3145–57.

**27.** Grutz G, Bucher K, Lavenir I, Larson R, Larson T, Rabbitts TH. The oncogenic T cell LIM-protein Lmo2 forms part of a DNA-binding complex specifically in immature T cells. EMBO J 1998;17:4594–605.

**28.** Nam CH, Rabbitts TH. The role of LMO2 in development and in T cell leukemia after chromosomal translocation or retroviral insertion. Mol Ther 2006;13: 15–25.

**29.** Vitelli L, Condorelli G, Lulli V, et al. A pentamer transcriptional complex including tal-1 and retinoblastoma protein downmodulates c-kit expression in normal erythroblasts. Mol Cell Biol 2000;20:5330–42.

**30.** Natkunam Y, Farinha P, Hsi ED, et al. LMO2 protein expression predicts survival in patients with diffuse large B-cell lymphoma treated with anthracycline-based chemotherapy with and without rituximab. J Clin Oncol 2008;26:447–54.

**31.** Natkunam Y, Zhao S, Mason DY, et al. The oncoprotein LMO2 is expressed in normal germinal-center B cells and in human B-cell lymphomas. Blood 2007;109:1636–42.

**32.** Lossos IS, Czerwinski DK, Alizadeh AA, et al. Prediction of survival in diffuse large-B-cell lymphoma based on the expression of six genes. N Engl J Med 2004; 350:1828–37.

**33.** Ma S, Guan XY, Beh PS, et al. The significance of LMO2 expression in the progression of prostate cancer. J Pathol 2007;211:278–85.

**34.** Wells JA, McClendon CL. Reaching for high-hanging fruit in drug discovery at protein-protein interfaces. Nature 2007;450:1001–9.

**35.** Tanaka T, Williams RL, Rabbitts TH. Tumour prevention by a single antibody domain inhibiting binding of signal transduction molecules to activated RAS. EMBO J 2007;26:3250–9.

**36.** Nam CH, Lobato MN, Appert A, Drynan LF, Tanaka T, Rabbitts TH. An antibody inhibitor of the LMO2-protein complex blocks its normal and tumorigenic functions. Oncogene 2008;27:4962–8.

**37.** Colas P, Cohen B, Jessen T, Grishina I, McCoy J, Brent R. Genetic selection of peptide aptamers that recognise and inhibit cyclin-dependent kinase 2. Nature 1996;380: 548–50.

**38.** Vojtek AB, Hollenberg SM. Ras-Raf interaction: two-hybrid analysis. Methods Enzymol 1995;255:331–42.

**39.** Sadowski I, Bell B, Broad P, Hollis M. GAL4 fusion vectors for expression in yeast or mammalian cells. Gene 1992;118:137–41.

**40.** Van Parijs L, Refaeli Y, Lord JD, Nelson BH, Abbas AK, Baltimore D. Uncoupling IL-2 signals that regulate T cell proliferation, survival, and Fas-mediated activation-induced cell death. Immunity 1999;11:281–8.

**41.** Morita S, Kojima T, Kitamura T. Plat-E: an efficient and stable system for transient packaging of retroviruses. Gene Ther 2000;7:1063–6.

**42.** Deane JE, Maher MJ, Langley DB, et al. Crystallization of FLINC4, an intramolecular LMO4-1 complex. Acta Crystallogr D Biol Crystallogr 2003;59:1484–6.

**43.** Deane JE, Ryan DP, Sunde M, et al. Tandem LIM domains provide synergistic binding in the LMO4:Ldb1 complex. EMBO J 2004;23:3589–98.

**44.** Rabbitts TH, Boehm T. LIM domains. Nature 1990; 346:418.

**45.** Boehm T, Foroni L, Kennedy M, Rabbitts TH. The rhombotin gene belongs to a class of transcriptional regulators with a potential novel protein dimerisation motif. Oncogene 1990;5:1103–5.

**46.** Ryan DP, Duncan JL, Lee C, Kuchel PW, Matthews JM. Assembly of the oncogenic DNA-binding complex LMO2–1-TAL1–12. Proteins 2008;70:1461–74.

**47.** Lahlil R, Lecuyer E, Herblot S, Hoang T. SCL assembles a multifactorial complex that determines glycophorin A expression. Mol Cell Biol 2004;24:1439–52.

**48.** McCormack MP, Rabbitts TH. Activation of the T-cell oncogene *LMO2* after gene therapy for X-linked severe combined immunodeficiency. N Engl J Med 2004;350: 913–21.

# Targeting LMO2 with a Peptide Aptamer Establishes a Necessary Function in Overt T-Cell Neoplasia

Alex Appert, Chang-Hoon Nam, Natividad Lobato, et al.

*Cancer Res* 2009;69:4784-4790.